

# Altered kinetics of nonhomologous end joining and class switch recombination in ligase IV-deficient B cells

Li Han and Kefei Yu

Department of Microbiology and Molecular Genetics, Michigan State University, East Lansing, MI 48824

**Immunoglobulin heavy chain class switch recombination (CSR) is believed to occur through the generation and repair of DNA double-strand breaks (DSBs) in the long and repetitive switch regions. Although implied, the role of the major vertebrate DSB repair pathway, nonhomologous end joining (NHEJ), in CSR has been controversial. By somatic gene targeting of DNA ligase IV (Lig4; a key component of NHEJ) in a B cell line (CH12F3) capable of highly efficient CSR in vitro, we found that NHEJ is required for efficient CSR. Disruption of the Lig4 gene in CH12F3 cells severely inhibits the initial rate of CSR and causes a late cell proliferation defect under cytokine stimulation. However, unlike V(D)J recombination, which absolutely requires NHEJ, CSR accumulates to a substantial level in Lig4-null cells. The data revealed a fast-acting NHEJ and a slow-acting alternative end joining of switch region breaks during CSR.**

CORRESPONDENCE  
Kefei Yu:  
yuke@msu.edu

DNA double-strand breaks (DSBs) are considered by many to be the most severe form of DNA damage, and are repaired by either homologous recombination or nonhomologous end joining (NHEJ). NHEJ is the primary DSB repair pathway in mammalian cells (1). A characteristic feature of NHEJ is the lack of long stretches of homology at the site of joining (junction), although a few base pairs of microhomology (nucleotides that can be assigned to either of the two DNA ends) are seen at 10–40% of junctions (2). The core components of the NHEJ pathway have been well characterized over the last decade. These include DNA end-binding complex Ku70–Ku80, DNA-dependent protein kinase (DNA-PKcs), Artemis, and the ligase complex x-ray cross complementation (XRCC) 4–DNA ligase IV (Lig4). Several accessory factors, including an XRCC4-like factor (known as XLF or Cernunnos) and polymerases  $\mu$  and  $\lambda$ , were identified in the following years. However, when NHEJ is disrupted by mutations to its core components, many forms of DSBs can still be joined, suggesting the existence of an alternative route for end joining.

During lymphocyte development, physiological DSBs arise as critical intermediates in V(D)J and class switch recombination (CSR). V(D)J recombination is a site-specific DNA recombination that assembles the antigen-binding

domain of Ig and T cell receptor genes. The RAG protein complex recognizes recombination signal sequences (RSS) next to the V, D, or J coding segments and cleaves the DNA at the RSS-coding sequence junction. A concerted cleavage of a pair of RSS generates four DNA ends that are joined to form a coding joint and a signal joint, respectively. CSR changes the constant domain of the Ig heavy chain, which allows a B cell to switch from expressing IgM to another isotype (IgG, IgA, or IgE). CSR is directed by kilobase-long repetitive switch regions ( $S\mu$ ,  $S\gamma$ ,  $S\alpha$ , and  $S\epsilon$ ) lying upstream of each constant region and requires activation-induced cytidine deaminase (AID). The preponderant experimental evidence is consistent with a cut-and-paste mechanism in a way similar to that of V(D)J recombination (3). First, the deleted region is circularized before its disposal. Second, DSBs were detected in switching B cells by ligation-mediated PCR. Third, phosphorylated histone H2AX (a marker for chromosomal breaks) foci were detected in switching B cells at the IgH locus in an AID-dependent manner. Finally, switch junctions show little

© 2008 Han and Yu. This article is distributed under the terms of an Attribution-Noncommercial-Share Alike-No Mirror Sites license for the first six months after the publication date (see <http://www.jem.org/misc/terms.shtml>). After six months it is available under a Creative Commons License (Attribution-Noncommercial-Share Alike 3.0 Unported license, as described at <http://creativecommons.org/licenses/by-nc-sa/3.0/>).

or no homology, consistent with direct joining of switch region breaks through NHEJ. Although the exact mechanism for switch region breaks remains unclear, the current view is that AID catalyzes cytidine deamination (converts cytidines to uracils) in the switch regions, followed by the repair of uracils that ultimately results in DSBs (3).

In contrast to V(D)J recombination, which absolutely requires NHEJ, direct testing of the role of NHEJ in CSR has met with considerable challenge. One obvious obstacle is that NHEJ-deficient animals cannot generate mature lymphocytes necessary for a CSR assay because the V(D)J recombination defect blocks T and B cell development. To circumvent the developmental block on B cells, *Ku*- or *DNA-PKcs*-deficient mice have been crossed with mice harboring preassembled Ig heavy and light chain genes to generate monoclonal NHEJ-deficient B cells (4–7). By this method, CSR was found completely abolished in the absence of Ku70 or Ku80 (4, 5). However, this conclusion must be interpreted with caution, because *Ku* may have non-NHEJ-related functions (e.g., telomere maintenance) and *Ku* deficiency causes defective cell proliferation (4, 5). As for *DNA-PKcs*, controversial results were obtained between a point mutation that inactivates *DNA-PKcs* and a complete deletion of the gene (6, 7). Although catalytically inactive *DNA-PKcs* allows normal CSR (7), deletion of the *DNA-PKcs* gene inhibited CSR to all isotypes except IgG1 (6). A caveat of this approach is that there are no T cells in the B cell–reconstituted mice. As a result, these mice have greatly reduced B cell numbers (4–6) and the B cells are inactive (8). The importance of T cell regulation was demonstrated by a later study showing restored CSR in *DNA-PKcs*-null mice upon T cell transplantation from a B cell-deficient host (8).

In contrast to *Ku* and *DNA-PKcs*, *XRCC4* and *Lig4* have no identified function outside NHEJ and their inactivation results in the most severe form of NHEJ deficiency. Therefore, *XRCC4* and *Lig4* are the most suitable and specific targets for abolishing NHEJ. However, the B cell reconstitution strategy is not feasible for *XRCC4* or *Lig4* because deletion of either gene in mice results in embryonic lethality (9, 10). Although p53 deficiency can extend the life of *XRCC4* and *Lig4* knockout mice, they all succumb to pro-B cell lymphomas shortly after birth (11, 12). Recently, two independent studies used conditional knockout methods to delete *XRCC4* in mature B cells (13, 14). Both studies found that CSR was reduced but not abolished in the absence of *XRCC4*. It is known that *XRCC4*-deficient cells have a very low level of *Lig4*. However, it was also reported that even a very low level of *Lig4* is still sufficient for NHEJ (15).

To unequivocally determine the role of NHEJ in CSR while avoiding the complications associated with some of the animal models, we disrupted the *Lig4* gene in a B cell line (CH12F3) capable of highly efficient cytokine-induced CSR in vitro (16). Like its parental line CH12.LX (17, 18), CH12F3 has a mostly stable diploid genome and is thus suitable for gene targeting. We chose to disrupt the *Lig4* gene not only because of its central role in NHEJ but also because it is dispensable for somatic cell growth (19). We found that deletion of *Lig4* in CH12F3 cells mildly reduced CSR after 3 d of cytokine stimulation, which is qualitatively and quantitatively similar to what was observed with *XRCC4*-deficient B cells, as well as the *Lig4*<sup>−/−</sup> *p53*<sup>−/−</sup> B cells (13, 14). However, we also found a proliferation defect of *Lig4*-null CH12F3 cells in the presence of cytokine stimulation. This led us to another important finding that the initial rate of CSR is severely inhibited in *Lig4*-null cells. Thus, the initially observed mild reduction appears to be an underestimation of a marked CSR defect, which is masked by an enrichment of switched cells. These observations reveal the kinetics of a fast-acting NHEJ and a slow-acting alternative end joining during CSR.

## RESULTS AND DISCUSSION

### Gene targeting of the *Lig4* gene in CH12F3 cells

*Lig4* is essential for mouse embryo development but dispensable for somatic cell growth. To determine the role of *Lig4* in CSR, we disrupted the *Lig4* gene on both alleles in CH12F3 cells. Mouse *Lig4* has a total of 911 amino acids. The entire coding sequence is located within the second exon. We replaced 78% of the *Lig4* coding region with a floxed puromycin marker (Fig. 1 A). The deleted region encodes amino acids 220–911, which contain the catalytic domain and the two BRCT motifs. This created a larger deletion than a previously defined null allele (10).

Six independent clones harboring a correctly targeted allele (designated L4 +/P) were obtained from a total of 192 puromycin-resistant clones. One of these was randomly selected for gene targeting of the second allele. First, the puromycin marker was excised by the Cre-LoxP reaction (designated L4 +/Δ). Then, the same targeting vector was used again to disrupt the second allele. One correctly targeted clone (designated L4 P/Δ) was obtained from a total of 34 puromycin-resistant clones (Fig. 1).

Because NHEJ deficiency is known to result in cellular hypersensitivity to DSB-inducing agents such as ionizing radiation and bleomycin, we tested the *Lig4*-null CH12F3 cells for this property. As expected, *Lig4*-null cells exhibited a marked sensitivity to zeocin (a bleomycin analogue; Fig. 1 C), based on a colorimetric assay that measures the metabolic conversion of thiazolyl blue tetrazolium bromide (MTT) in the mitochondria of living cells (20).

### Reduced CSR in *Lig4*-null cells

To determine the CSR capacity of *Lig4*-null CH12F3 cells, cells were seeded at a low density ( $5 \times 10^4$  cells/ml) and grown in the presence of cytokines for 72 h, as previously described (see Materials and methods) (16). CSR in *Lig4*-null cells is reduced to ~40–50% of that of the *Lig4*-heterozygous cells (Fig. 2, A and B), which are indistinguishable from wild-type cells (not depicted). This is consistent with the two recent studies (13, 14) showing a similar reduction of CSR in *XRCC4*-deficient mouse primary B cells and in *Lig4*<sup>−/−</sup> *p53*<sup>−/−</sup> B cells, indicating the existence of alternative end joining that can resolve switch region breaks.

To confirm that the reduction was indeed caused by a *Lig4* deficiency rather than a clonal effect, a genetic complementation assay was performed. First, the floxed puromycin marker in L4 P/Δ cells was excised by the Cre-LoxP reaction to generate puromycin-sensitive *Lig4*-null cells (designated L4 Δ/Δ; Fig. 2 C). Then, L4 Δ/Δ cells were infected with recombinant retroviruses expressing the mouse *Lig4* or control virus made from the empty vector. Infected cells were selected by puromycin and subjected to the CSR analysis. As shown in Fig. 2 D, *Lig4*-transduced cells had restored normal levels of CSR, but the cells transduced with the control virus did not.

#### Altered kinetics of CSR in *Lig4*-null cells

Because CSR is regulated by cell division, we analyzed the effect of *Lig4* deletion on cell proliferation. *Lig4*-null CH12F3 cells propagated normally without cytokine stimulation (Fig. 3 A, left). However, slower propagation of *Lig4*-null cells was detected at 48 and 72 h in the presence of cytokines (Fig. 3 A, right). To distinguish whether this was caused by a reduced proliferation rate or increased cell death, we stained the cells with CFSE and monitored cell divisions through the passive dilution of CFSE. Although the CFSE fluorescence profiles of *Lig4*-heterozygous and *Lig4*-null cells completely overlap in the absence of cytokines (Fig. 3 B, left column), a shift toward brighter CFSE was observed for *Lig4*-null cells in the presence of cytokines at 48 and 72 h (Fig. 3 B, right column), indicating reduced proliferation. We next analyzed cell death using FITC-conjugated annexin V and propidium iodide (PI), which stain early apoptotic and dead cells, respectively. No significant difference in apoptosis or cell death was observed for the two genotypes in the absence of cytokines (Fig. 3 C). However, an increase of apoptosis or cell death

(left). However, slower propagation of *Lig4*-null cells was detected at 48 and 72 h in the presence of cytokines (Fig. 3 A, right). To distinguish whether this was caused by a reduced proliferation rate or increased cell death, we stained the cells with CFSE and monitored cell divisions through the passive dilution of CFSE. Although the CFSE fluorescence profiles of *Lig4*-heterozygous and *Lig4*-null cells completely overlap in the absence of cytokines (Fig. 3 B, left column), a shift toward brighter CFSE was observed for *Lig4*-null cells in the presence of cytokines at 48 and 72 h (Fig. 3 B, right column), indicating reduced proliferation. We next analyzed cell death using FITC-conjugated annexin V and propidium iodide (PI), which stain early apoptotic and dead cells, respectively. No significant difference in apoptosis or cell death was observed for the two genotypes in the absence of cytokines (Fig. 3 C). However, an increase of apoptosis or cell death

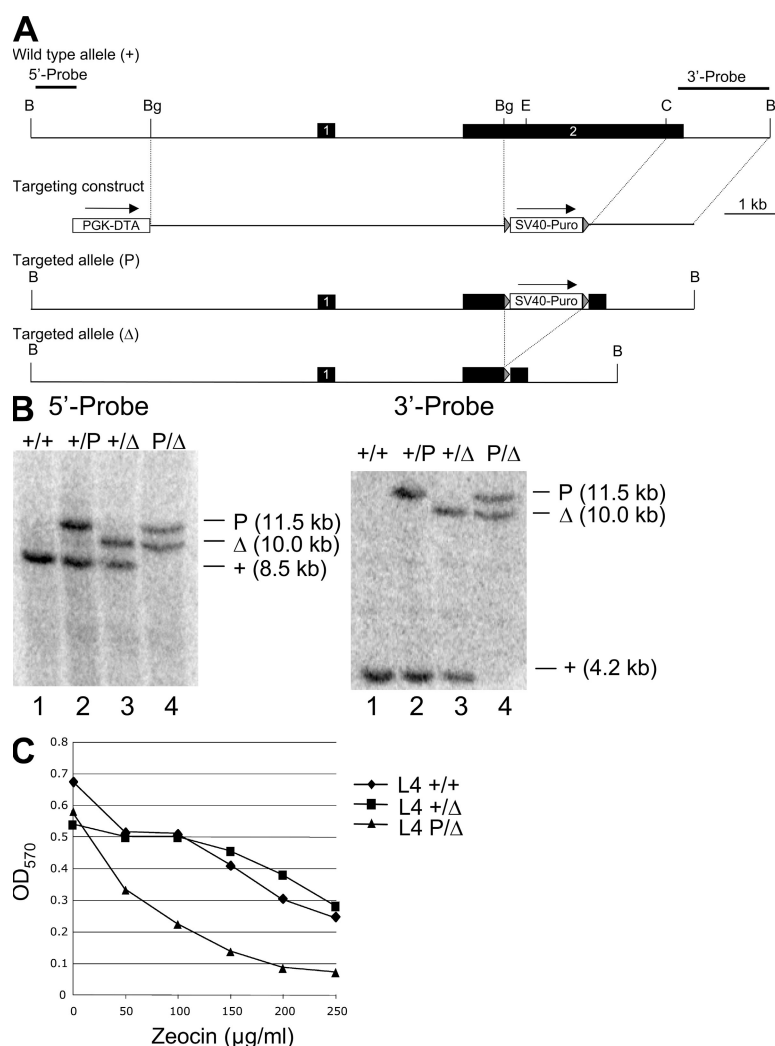


**Figure 1. Gene targeting of *Lig4* in CH12F3 cells.** (A) Genomic organization of wild-type and targeted mouse *Lig4* locus. Closed boxes indicate exons. Small triangles indicate lox P sites. Restriction enzyme sites: B, Bam HI; Bg, Bgl II; C, Cla I; E, EcoR V. DTA, diphtheria toxin A chain; PGK, phosphoglycerate kinase promoter; Puro, puromycin resistance gene; SV40, SV40 early promoter. (B) Southern blot analysis of Bam HI- and EcoR V-digested genomic DNA. Genotype symbols: +, wild-type allele; P and Δ, targeted allele with or without the puro-selectable marker, respectively. (C) Cellular sensitivity to zeocin as determined by the MTT assay. Higher absorbance indicates more live cells in the culture.

was observed in *Lig4*-null culture in the presence of cytokines at 48 and 72 h (Fig. 3 C). This suggests that diminished repair capacity in *Lig4*-null cells leads to elevated apoptosis triggered by CSR-associated DSB.

The growth difference of *Lig4*-heterozygous and *Lig4*-null cells in the presence of cytokines prompted us to reevaluate the mild effect of *Lig4* deletion initially observed on CSR. Two possible mechanisms could account for the reduction of CSR in the absence of *Lig4*. One possibility is that *Lig4* affects cell proliferation in a way unrelated to NHEJ, which in turn affects CSR. The other explanation is that *Lig4* is essential for efficient repair of switch region breaks. Without *Lig4*, accumulation of switch region breaks cause cell-cycle arrest, which is manifested as a cell proliferation defect. If the former were true, CSR level between the two genotypes (*L4* +/Δ vs. P/Δ) should be similar at 24 h, as cell proliferation is apparently the same (Fig. 3 A, right). However, if the latter were true, CSR difference between the two genotypes (*L4* +/Δ vs. P/Δ) should be more significant at the beginning before the elimination of CSR-failed cells (and the enrichment of switched cells).

To distinguish these two possibilities, a time course of CSR was performed. A representative experiment is shown in Fig. 4 A (left). Although the numerical value of CSR varies

slightly in different experiments, the relative ratio of CSR between the two genotypes (*L4* +/Δ vs. P/Δ) is consistent. At 24, 48, and 72 h, CSR of the *Lig4*-null cell was at 13, 29, and 48%, respectively, of that of the *Lig4*-heterozygous cell (Fig. 4 A, right). Continued subculturing (>7 d) of *Lig4*-null cells in the presence of cytokines eventually led to ~80–90% of the wild-type CSR level (unpublished data). CH12F3 cells grow rapidly in culture with an estimated doubling time of ~8–10 h. Seeding at a very low density is necessary to achieve maximum levels of CSR without subculturing. However, this condition is less optimal for accurately measuring the initial rate of CSR. Therefore, we also seeded the cells at  $3 \times 10^5$  cells/ml (early log phase) and measured CSR after 24 h. Again, a marked reduction of CSR in *Lig4*-null cells was observed (15% of wild-type level; Fig. 4 B, right) despite a comparable rate of cell proliferation (Fig. 4 B, left). Thus, the optimal rate of CSR requires *Lig4* regardless of stimulation conditions.

These data support the hypothesis that NHEJ is the primary repair mechanism for switch region breaks. The small endpoint reduction observed initially is likely an underestimation of a marked CSR defect, which is probably masked by an enrichment of IgA cells that have managed to repair their switch region breaks through alternative end joining.

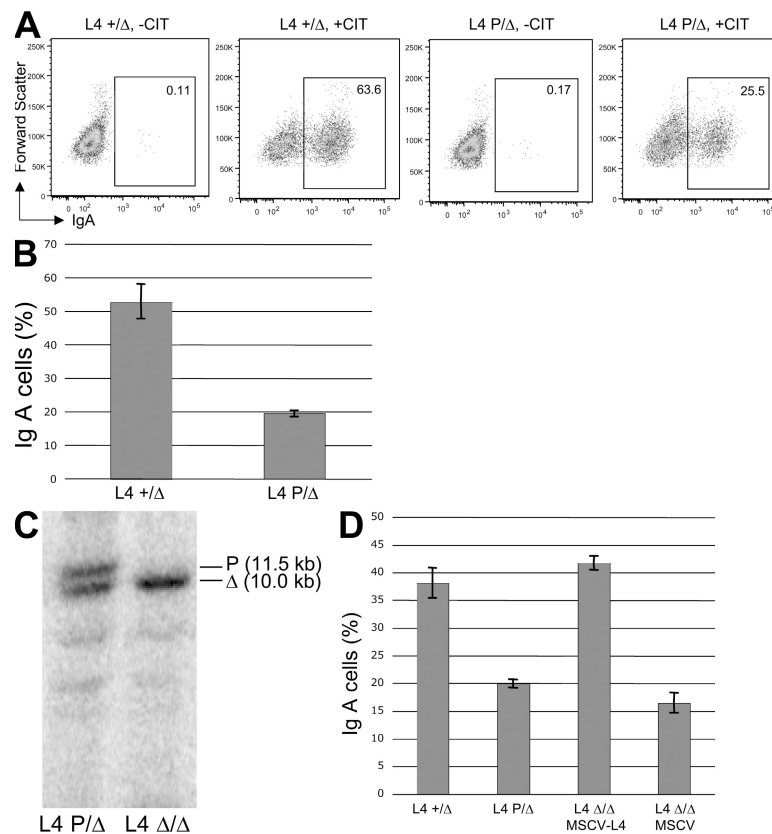


**Figure 2. Reduced CSR in *Lig4*-null cells.** (A) FACS analysis of CSR by surface staining of IgA after 72 h of cell growth with or without cytokines. Numbers in boxed areas indicate percentages. CIT, anti-CD40 antibody (IL-4 and TGF- $\beta$ 1). (B) Reduced CSR in *Lig4*-null B cells after 72 h of cytokine stimulation. Error bars represent standard deviations from three independent experiments. (C) Southern blot analysis of Cre-mediated excision of puro resistance marker in *Lig4*-null cells. (D) Genetic complementation of CSR defect in *Lig4*-null cells by retroviral transduction of *Lig4*. Error bars represent standard deviations from three independent experiments.

Nevertheless, in the absence of NHEJ, alternative end joining can effectively repair switch region breaks, albeit at a substantially slower rate.

### Switch junction sequences

Numerous studies have shown increased use of microhomology at the junctions in NHEJ-deficient cells (14, 21, 22). To

determine whether switch junctions in *Lig4*-null cells are microhomology mediated, we cloned and sequenced  $\text{S}\mu$ - $\text{S}\alpha$  junctions from stimulated *Lig4*-heterozygous and *Lig4*-null cells. Because  $\text{S}\alpha$  is highly homologous to  $\text{S}\mu$ , we chose to PCR amplify switch junctions from individual cell clones. Cloning individual switch junctions instead of amplifying from a pool of cells helps to eliminate false junctions produced by

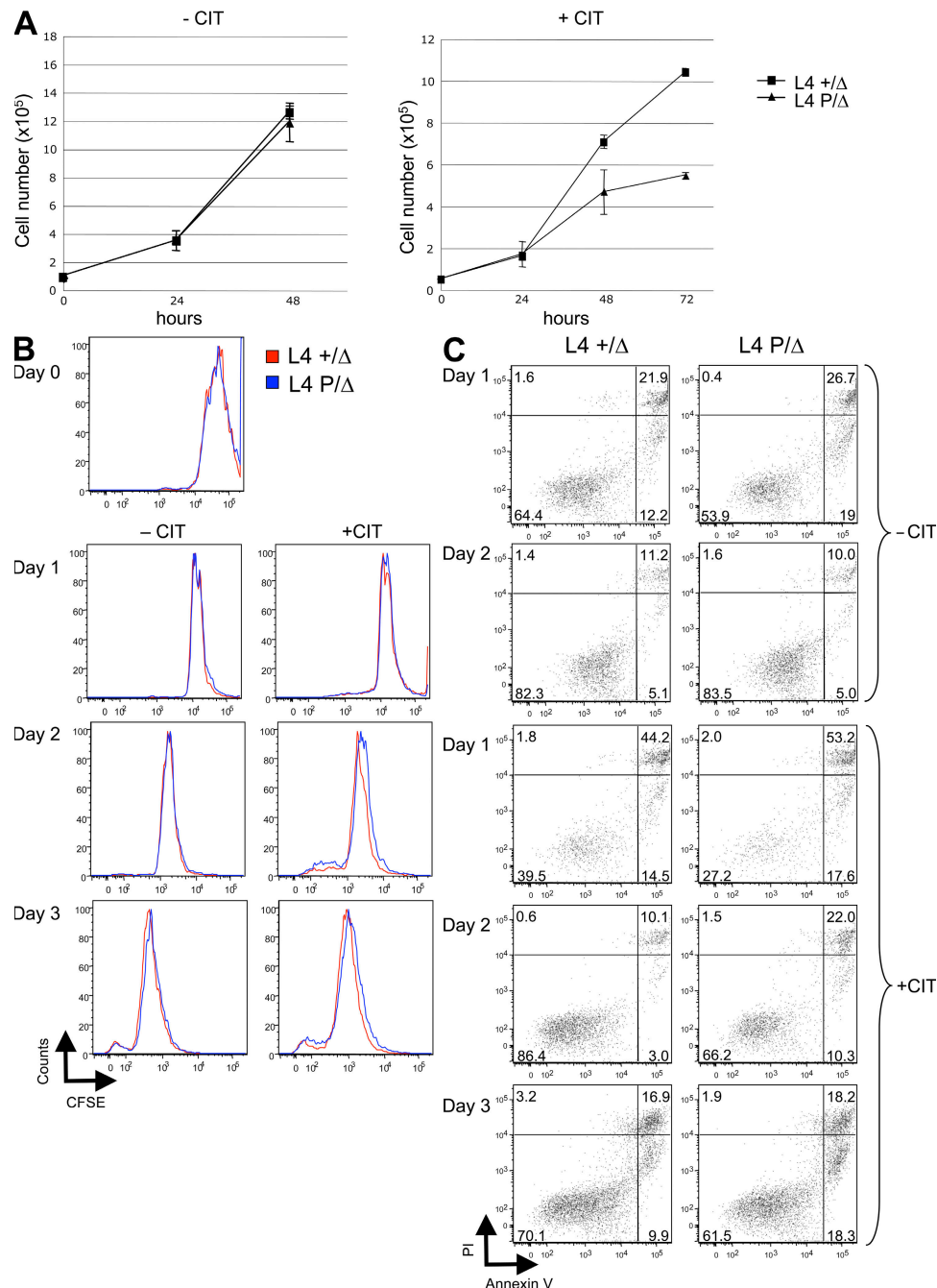


**Figure 3. Proliferation of *Lig4*-null cells.** (A) Normal and reduced propagation of *Lig4*-null cells in the absence (top) and presence (bottom) of cytokine stimulation, respectively. Error bars represent standard deviations from three independent experiments. (B) CFSE profiles of *Lig4*-heterozygous (red) and *Lig4*-null (blue) cells at every 24 h in the absence (left) and presence (right) of cytokines (CIT). (C) Early apoptosis (annexin V-FITC) and cell death (PI) at every 24 h in the absence and presence of cytokines (CIT). Numbers in boxed areas indicate percentages.

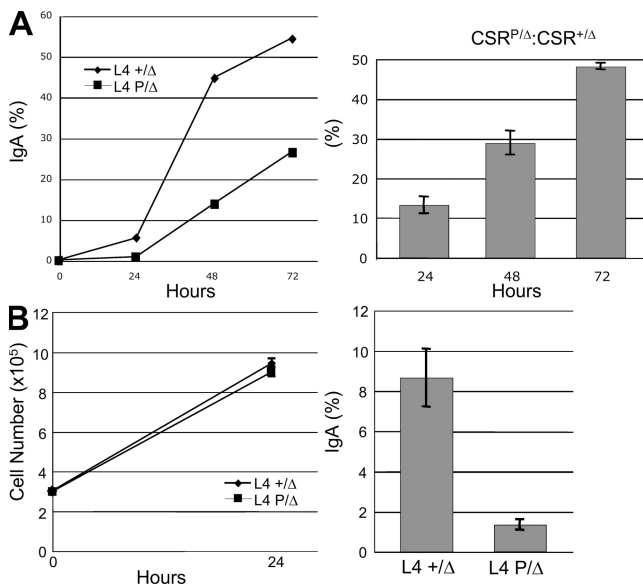


**Figure 4. Lig4 affects the rate of CSR.** (A, left) A representative time course of CSR between *Lig4*-heterozygous and *Lig4*-null cells. (right) Ratio of CSR between *Lig4*-heterozygous and *Lig4*-null cells after 24, 48, and 72 h of cytokine stimulation. (B) Proliferation (left) and initial rate of CSR (right) for cells seeded at early log phase density ( $3 \times 10^5$  cells/ml). Error bars represent standard deviations from three independent experiments.

template switching of stalled PCR intermediates, as well as the bias against large amplicons. In addition, the distinctive size of each PCR product was used to reference the authenticity of the sequenced junction. We found that 27% of the junctions from *Lig4*-heterozygous cells were direct joins, but there were none for the *Lig4*-null cells (Fig. 5). The difference is statistically significant (7 out of 26 vs. 0 out of 23; two-tail p-value of 0.01 by Fisher's exact test) and consistent with what was observed for the  $\text{S}\mu$ - $\text{S}\gamma$  switch junctions in *XRCC4*-deficient B cells (14). The distribution of recombination break points is indistinguishable between the two genotypes (unpublished data).

#### DNA end joining in CSR

This study highlights the importance of NHEJ as the primary mechanism of DSB repair in CSR but also reveals the flexibility of using alternative end joining, which is in sharp contrast to NHEJ-dependent V(D)J recombination. The mild endpoint reduction of CSR in *Lig4*-null CH12F3 cells is in agreement with two recent studies using a conditional knockout of *XRCC4* in mature B cells (13, 14). However, our study differs from those two regarding cell proliferation under cytokine stimulation. We found a reduced proliferation of *Lig4*-null cells at the late stage of stimulation, which was not obvious in the two *XRCC4* studies. Our observation would argue for a dominant role of NHEJ in CSR, whereas others would argue for the robustness of the alternative end joining. It should be noted that in one of the studies, deletion of *XRCC4* is incomplete (13). In the other study, cell prolif-

eration was measured on a *p53*-deficient background, which lacks the proper cell-cycle checkpoint control (14).

Although alternative NHEJ can efficiently join linearized plasmids, it clearly cannot replace NHEJ for V(D)J recombination or cellular resistance to ionizing radiation. One speculation has been that alternative end joining is not optimized for repair chromosomal breaks, which is not applicable in this case. Another view is that DSBs are repaired in a manner reflecting how they are generated. It is widely believed that the strict dependence of V(D)J recombination on NHEJ stems from the active guidance of the RAG proteins in the postcleavage complex (14, 22). Indeed, fusion of the RAG proteins to the I-Sce I endonuclease can direct I-Sce I breaks solely to NHEJ (23). On the other hand, certain *RAG* mutations can significantly alleviate the dependence of V(D)J recombination on NHEJ (22). Therefore, the flexibility of using alternative end joining in CSR might originate from the complete accessibility of AID-initiated breaks. Interestingly, a single I-Sce I break engineered at an acceptor switch region can efficiently support CSR (24), strongly suggesting that CSR does not require the type of synaptic complex presumed to exist in V(D)J recombination.

Alternative end joining was found to excessively use microhomology. Because all switch regions are abundant in conserved pentamer sequences (e.g., GAGCT and GGGGG/CT; underlining indicates one nucleotide position), these short sequences could potentially serve as homology blocks and promote the utilization of alternative end joining. Indeed, there was a marked shift toward microhomology-mediated joining in *Lig4*-null cells. The most remarkable observation was that there was no direct join in the absence of *Lig4*. This is in complete agreement with what has been observed for  $\text{S}\mu$ - $\text{S}\gamma$  junctions in *XRCC4*-deficient mouse B cells (13, 14) and in human patients harboring hypomorphic *Lig4* mutations (21).

Mammalian cells have three ATP-dependent DNA ligases (Lig1, 3, and 4). As a dedicated DSB repair enzyme, The Lig4 complex (XLF-XRCC4-Lig4) has a remarkable flexibility of joining blunt, compatible, and incompatible ends, and even ligating across a gap (25). In contrast, Lig1 and Lig3 are considered as nick ligases. However, recent studies have shown that Lig3 is also capable of intermolecular ligation of blunt and short compatible ends (25, 26). Although the exact architecture of alternative end joining remains unclear, biochemical evidence has suggested the XRCC1-Lig3 complex as a primary candidate for the ligation step (27, 28). Disruption of *Lig3* or *XRCC1* in mice causes embryonic lethality, thereby limiting their genetic characterizations in alternative end joining. However, Lig3 deficiency might not be cellularly lethal given that XRCC1-deficient cells are viable. In this regard, somatic gene targeting of *Lig3* might be a suitable way of dissecting the role of alternative end joining in CSR, as well as DSB repair in general in mammalian cells.

#### MATERIALS AND METHODS

**Cell culture and CSR assay.** CH12F3 cells were obtained from T. Honjo (Kyoto University, Kyoto, Japan). Cells were cultured as previously described (16). Cell propagation was analyzed by counting live cells every 24 h.



**Figure 5.  $\mu$ - $\sigma$  junction sequences.** (A) Percentage of switch junctions with the indicated length of microhomology (excluding nucleotide additions). (B and C) Alignment of switch junctions with germline sequences. Germline  $\mu$  (black) and  $\sigma$  (gray) sequences are listed on the top and bottom, respectively, of each junction sequence (blue). Microhomologies (boxes) are identified as the largest perfect matches to the germline sequences. Nucleotide additions are underlined. Long vertical lines indicate direct joins. Small vertical lines indicate identity between the junction and germline sequences. Several junctions containing inverted  $\mu$  are indicated by arrows.

Unless indicated otherwise in the figures, stimulation of CH12F3 cells was performed by seeding log phase cells at  $5 \times 10^4$  cells/ml in medium supplemented with 5% NCTC-109 medium, 1  $\mu$ g/ml anti-CD40 antibody, 5 ng/ml IL-4, and 0.5 ng/ml TGF- $\beta$ 1, and cells were grown for 72 h. Cells were stained with FITC-conjugated anti-mouse IgA antibody and analyzed by flow cytometry. Class switch efficiency was determined as the percentage of IgA-positive cells.

**Gene targeting.** The targeting vector backbone (pTV2DN2) was obtained from J. Mann (Murdoch Children's Research Institute, Parkville, Australia). A 6.1-kb Bgl II fragment (139,231–145,321) and a 1.8-kb Cla I-Bam HI fragment (148,114–149,923; both available from GenBank/EMBL/DDBJ under accession no. AC138397) from bacterial artificial chromosome clone RP23-65O11 were used as the two homology blocks for gene targeting. The relevant part of the targeting vector is shown in Fig. 1 A. 10 million CH12F3 cells were transfected with 10  $\mu$ g of linear targeting vector and seeded into five 96-well plates. Puromycin was added 48 h later to a final concentration of 1  $\mu$ g/ml. Puromycin-resistant clones were picked after 7–10 d and screened by PCR and Southern blot analysis.

**MTT assay.** Cells were seeded at  $2 \times 10^5$  cells/ml/well in a 24-well plate and grown for 48 h in various concentrations of zeocin. Metabolic conversion of MTT was performed by incubation of harvested cells in 1 mg/ml MTT (in 1× phosphate-based saline) for 2 h. The cell pellet was lysed in 100  $\mu$ l of acidic isopropanol (1 ml of concentrated hydrochloric acid in 349 ml isopropanol), and the absorbance was measured at 570 nm.

**Genetic complementation.** The *Lig4* coding region sequence was cloned into plasmid pMSCVpuro (Clontech Laboratories, Inc.). Recombinant retrovirus was made by transfection of pMSCV plasmids into retrovirus packaging cell line Phoenix (provided by the Nolan Laboratory, Stanford University, Palo Alto, CA). The viral supernatants were harvested and used to infect *Lig4*-null cells (L4  $\Delta/\Delta$ ). Infected cells were selected by puromycin and subjected to CSR assays.

**Cell proliferation and cell death analysis.** To monitor cell proliferation, cells were stained with 10 nM CFSE (Invitrogen) for 15 min at 37°C and washed three times with ice-cold growth medium. CFSE intensity was measured every 24 h. For detection of early apoptotic and dead cells, cells were stained with FITC-conjugated annexin V and PI and analyzed every 24 h until the culture reached confluence.

**Switch junction analysis.** Individual IgA-positive clones were isolated by limited dilutions of cytokine-stimulated cultures in 96-well plates. Switch junctions were amplified with primers KY761 (5'-AACTCTCCAGCCACAG-TAATGACC-3') and KY743 (5'-GAGCTCGTGGAGTGTCAAGT-3'). The PCR product was sequenced at the Genomic Core Facility of Michigan State University.

We thank Dr. T. Honjo for providing CH12F3 cells, Dr. J. Mann for plasmids and advice on gene targeting, and Dr. C.-L. Hsieh for cytogenetic analysis of CH12F3 cells. We are indebted to Dr. K. Meek for discussion and critical review of the manuscript. Christina Brownlee provided technical assistance.

The authors have no conflicting financial interests.

**Submitted:** 24 July 2008

**Accepted:** 16 October 2008

## REFERENCES

1. Lieber, M.R. 1998. Warner-Lambert/Parke-Davis Award Lecture. Pathological and physiological double-strand breaks: roles in cancer, aging, and the immune system. *Am. J. Pathol.* 153:1323–1332.
2. Lieber, M.R. 2008. The mechanism of human nonhomologous DNA end joining. *J. Biol. Chem.* 283:1–5.
3. Chaudhuri, J., and F.W. Alt. 2004. Class-switch recombination: interplay of transcription, DNA deamination and DNA repair. *Nat. Rev. Immunol.* 4:541–552.
4. Manis, J.P., Y. Gu, R. Lansford, E. Sonoda, R. Ferrini, L. Davidson, K. Rajewsky, and F.W. Alt. 1998. Ku70 is required for late B cell development and immunoglobulin heavy chain class switching. *J. Exp. Med.* 187:2081–2089.
5. Casellas, R., A. Nussenzweig, R. Wuerffel, R. Pelanda, A. Reichlin, H. Suh, X.F. Qin, E. Besmer, A. Kenter, K. Rajewsky, and M.C. Nussenzweig. 1998. Ku80 is required for immunoglobulin isotype switching. *EMBO J.* 17:2404–2411.
6. Manis, J.P., D. Dudley, L. Kaylor, and F.W. Alt. 2002. IgH class switch recombination to IgG1 in DNA-PKcs-deficient B cells. *Immunity*. 16:607–617.
7. Bosma, G.C., J. Kim, T. Urich, D.M. Fath, M.G. Cotticelli, N.R. Ruetsch, M.Z. Radic, and M.J. Bosma. 2002. DNA-dependent protein kinase activity is not required for immunoglobulin class switching. *J. Exp. Med.* 196:1483–1495.
8. Kiefer, K., J. Oshinsky, J. Kim, P.B. Nakajima, G.C. Bosma, and M.J. Bosma. 2007. The catalytic subunit of DNA-protein kinase (DNA-PKcs) is not required for Ig class-switch recombination. *Proc. Natl. Acad. Sci. USA*. 104:2843–2848.
9. Barnes, D.E., G. Stamp, I. Rosewell, A. Denzel, and T. Lindahl. 1998. Targeted disruption of the gene encoding DNA ligase IV leads to lethality in embryonic mice. *Curr. Biol.* 8:1395–1398.
10. Frank, K.M., J.M. Sekiguchi, K.J. Seidl, W. Swat, G.A. Rathbun, H.L. Cheng, L. Davidson, L. Kangaloo, and F.W. Alt. 1998. Late embryonic lethality and impaired V(D)J recombination in mice lacking DNA ligase IV. *Nature*. 396:173–177.
11. Gao, Y., D.O. Ferguson, W. Xie, J.P. Manis, J. Sekiguchi, K.M. Frank, J. Chaudhuri, J. Horner, R.A. DePinho, and F.W. Alt. 2000. Interplay of p53 and DNA-repair protein XRCC4 in tumorigenesis, genomic stability and development. *Nature*. 404:897–900.
12. Frank, K.M., N.E. Sharpless, Y. Gao, J.M. Sekiguchi, D.O. Ferguson, C. Zhu, J.P. Manis, J. Horner, R.A. DePinho, and F.W. Alt. 2000. DNA ligase IV deficiency in mice leads to defective neurogenesis and embryonic lethality via the p53 pathway. *Mol. Cell*. 5:993–1002.
13. Soulas-Sprauel, P., G. Le Guyader, P. Rivera-Munoz, V. Abramowski, C. Olivier-Martin, C. Goujet-Zalc, P. Charneau, and J.P. de Villartay. 2007. Role for DNA repair factor XRCC4 in immunoglobulin class switch recombination. *J. Exp. Med.* 204:1717–1727.
14. Yan, C.T., C. Boboila, E.K. Souza, S. Franco, T.R. Hickernell, M. Murphy, S. Gumaste, M. Geyer, A.A. Zarrin, J.P. Manis, et al. 2007. IgH class switching and translocations use a robust non-classical end-joining pathway. *Nature*. 449:478–482.
15. Windhofer, F., W. Wu, and G. Iliakis. 2007. Low levels of DNA ligases III and IV sufficient for effective NHEJ. *J. Cell. Physiol.* 213:475–483.
16. Nakamura, M., S. Kondo, M. Sugai, M. Nazarea, S. Imamura, and T. Honjo. 1996. High frequency class switching of an IgM+ B lymphoma clone CH12F3 to IgA+ cells. *Int. Immunol.* 8:193–201.
17. Ukai, A., T. Maruyama, S. Mochizuki, R. Ouchida, K. Masuda, K. Kawamura, M. Tagawa, K. Kinoshita, A. Sakamoto, T. Tokuhisa, and J.-O.-Wang. 2006. Role of DNA polymerase theta in tolerance of endogenous and exogenous DNA damage in mouse B cells. *Genes Cells*. 11:111–121.
18. Hostager, B.S., S.A. Haxhinasto, S.L. Rowland, and G.A. Bishop. 2003. Tumor necrosis factor receptor-associated factor 2 (TRAF2)-deficient B lymphocytes reveal novel roles for TRAF2 in CD40 signaling. *J. Biol. Chem.* 278:45382–45390.
19. Grawunder, U., D. Zimmer, S. Fugmann, K. Schwarz, and M.R. Lieber. 1998. DNA ligase IV is essential for V(D)J recombination and DNA double-strand break repair in human precursor lymphocytes. *Mol. Cell*. 2:477–484.
20. Mosmann, T. 1983. Rapid colorimetric assay for cellular growth and survival: application to proliferation and cytotoxicity assays. *J. Immunol. Methods*. 65:55–63.
21. Pan-Hammarstrom, Q., A.M. Jones, A. Lahdesmaki, W. Zhou, R.A. Gatti, L. Hammarstrom, A.R. Gennery, and M.R. Ehrenstein. 2005. Impact of DNA ligase IV on nonhomologous end joining pathways during class switch recombination in human cells. *J. Exp. Med.* 201:189–194.
22. Corneo, B., R.L. Wendland, L. Deriano, X. Cui, I.A. Klein, S.Y. Wong, S. Arnal, A.J. Holub, G.R. Weller, B.A. Pancake, et al. 2007. Rag mutations reveal robust alternative end joining. *Nature*. 449:483–486.

23. Cui, X., and K. Meek. 2007. Linking double-stranded DNA breaks to the recombination activating gene complex directs repair to the non-homologous end-joining pathway. *Proc. Natl. Acad. Sci. USA.* 104: 17046–17051.
24. Zarrin, A.A., C. Del Vecchio, E. Tseng, M. Gleason, P. Zarin, M. Tian, and F.W. Alt. 2007. Antibody class switching mediated by yeast endonuclease-generated DNA breaks. *Science.* 315:377–381.
25. Gu, J., H. Lu, B. Tippin, N. Shimazaki, M.F. Goodman, and M.R. Lieber. 2007. XRCC4:DNA ligase IV can ligate incompatible DNA ends and can ligate across gaps. *EMBO J.* 26:1010–1023.
26. Cotter-Gohara, E., I.K. Kim, A.E. Tomkinson, and T. Ellenberger. 2008. Two DNA-binding and nick recognition modules in human DNA ligase III. *J. Biol. Chem.* 283:10764–10772.
27. Wang, H., B. Rosidi, R. Perrault, M. Wang, L. Zhang, F. Windhofer, and G. Iliakis. 2005. DNA ligase III as a candidate component of backup pathways of nonhomologous end joining. *Cancer Res.* 65:4020–4030.
28. Audebert, M., B. Salles, and P. Calsou. 2004. Involvement of poly(ADP-ribose) polymerase-1 and XRCC1/DNA ligase III in an alternative route for DNA double-strand breaks rejoining. *J. Biol. Chem.* 279: 55117–55126.